Journal of Physics: Conference Series **67** (2007) 012003 doi:10.1088/1742-6596/67/1/012003

Schrödinger-cat states and decoherence in quantum-electromechanical systems

Maximilian Schlosshauer

Department of Physics, University of Melbourne, Victoria, 3010, Australia

E-mail: m.schlosshauer@unimelb.edu.au

Abstract.

Quantum-electromechanical systems are nanoscale mechanical resonators whose high-frequency oscillations are detected by an electronic transducer. Despite their macroscopic size and mechanical, ordinary-matter nature, these resonators can exhibit distinct quantum behavior that is of great interest and promise to an experimental exploration of questions in the foundations of quantum mechanics. After a brief introduction to quantum-electromechanical systems, I will sketch the feasibility and features of superposition states of macroscopically distinct positions in such systems. I will also show how these systems give rise to a new and hitherto hardly explored decoherence model and present some first results for this model.

1. Introduction

Quantum-electromechanical systems (QEMS) are relatively new players on the fascinating field of experiments that explore the limits of quantum mechanics. QEMS show great promise for the demonstration of truly mechanical "Schrödinger kittens" and for experimental tests of decoherence models and (possibly) physical collapse theories. It is quite reasonable to expect that QEMS will very soon be indelibly linked to foundational topics, such as the measurement problem, entanglement, nonlocality, decoherence, and the like. For anybody working in the foundations of quantum mechanics, a basic familiarity with these rather novel and fascinating quantum systems should therefore prove useful. In this paper, I shall give such a "foundations-minded" introduction to QEMS, focusing on a few selected aspects.

Over the past decade an astonishing array of experiments has pushed the quantum–classical boundary far into the quantum domain. The creation, manipulation, and detection of quantum superpositions of macroscopically distinguishable states has begun to give experimental relevance and underpinning to the initially pure *Gedanken* character of Schrödinger's famous cat "paradox" [1]. For example, the existence of superpositions of μA currents running in opposite directions has been confirmed in superconducting interference devices (SQUIDs) [2, 3], and spatial interference patterns of the double-slit type have been observed for massive C_{70} fullerenes and biomolecules [4, 5, 6]. (For an overview of these and other recent experiments on superpositions of macroscopically distinct states, see, e.g., [7].) The experiments clearly demonstrate the fuzziness of the quantum–classical boundary, with decoherence – the local loss of quantum coherence due to ubiquituous interactions with the environment [8, 9, 10, 11, 12, 13] – providing a purely quantum-mechanical explanation for why it is so difficult to observe such "Schrödinger kittens." Decoherence supplies a universal qualitative and formal description of

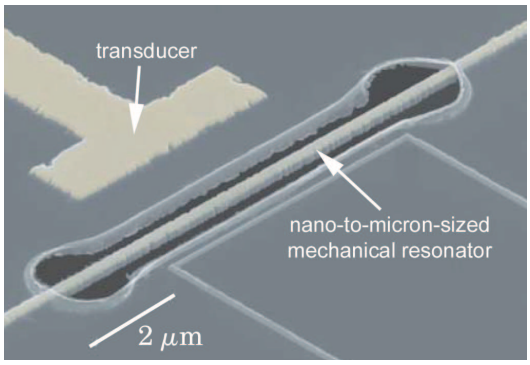

Figure 1. Example for the experimental realization of a QEMS from the laboratory of Keith Schwab at Cornell University. A doubly clamped beam ("bridge") serves as the nanomechanical resonator whose vibrational motion is translated into an electrical signal by means of an electronic transducer (such as a single-electron transistor).

the quantum-to-classical transition and provides a rigorous quantitative measure for determining the location of the boundary at which this transition occurs.

QEMS are a direct product of the recent revolution in nanotechnology. The vast possibilities of, and immense potential inherent in, a miniaturization of physical structures down to microscales and nanoscales was already envisioned in Feynman's famous speech of 1959 entitled "There is plenty of room at the bottom." The core component of a QEMS is a tiny mechanical resonator in form of a suspended beam, with typical dimensions on the scale of nanometers and micrometers and usually manufactured from crystalline materials such as Si (Fig. 1). The beam can either be clamped to the surrounding substrate on only one end (cantilever) or on both ends (bridge; see Fig. 1). Through the brief application of a suitable driving force, the beam is set into an oscillatory motion. This motion is in turn detected by a electronic transducer, such as a single-electron transistor capacitatively coupled to the beam, and converted into an electrical signal that can be read out in order to observe the beam's motion.

Due to the small spatial dimensions, the natural frequency of QEMS resonators can be made very large. Recent experiments have achieved frequencies in the GHz range [14]. In other words, QEMS represent mechanical structures oscillating at radio and microwave frequencies! Another striking feature of these nanomechanical resonators is their large quality (or "Q") factor: The resonators typically perform tens of thousands of free oscillations before the amplitude becomes noticeably damped due to dissipative effects.

Most interestingly, though, despite their macroscopic size (typical nanomechanical resonators contain billions of atoms!), the resonators can exhibit distinct quantum effects, motivating the first letter in the acronym "QEMS." First off, given the large number of atoms present in the resonator, it would appear that a similiarly large number of vibrational degrees of freedom would need to be taken account. However, it turns out that in practice only the lowest fundamental flexural mode of the beam is relevant. All other modes are either "frozen out" (QEMS are typically operated at very low temperatures close to absolute zero), or their coupling to the transducer is negligibly weak. This brings about an important simplification: The nanomechanical resonator can effectively be treated as a single quantum-mechanical harmonic oscillator!

What are the different forms of (observed or predicted) quantum behavior in QEMS? One important feature of QEMS is their extreme senstivity to spatial displacements. A key quantity is here the so-called (quantum) zero-point displacement uncertainty $\Delta x_{\rm zp}$ of the harmonic

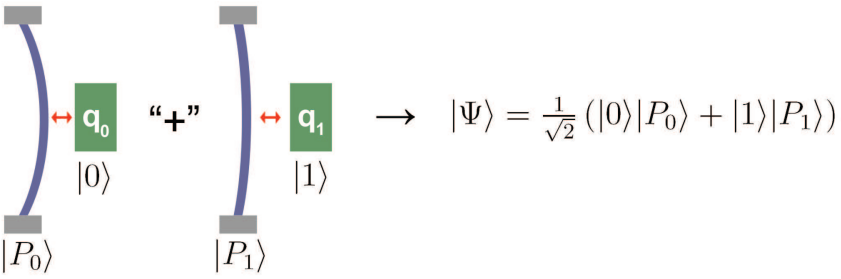

Figure 2. Scheme for the creation of a spatial "cat state" in QEMS, as proposed by Armour, Blencowe, and Schwab [18]. A Cooper-pair box, described by basis states $|0\rangle$ and $|1\rangle$ (corresponding to charges q_0 and q_1, respectively, on the superconducting island of the box), is electrostatically coupled to the nanomechanical beam (blue). Preparation of the box in a coherent superposition $\frac{1}{\sqrt{2}}(|0\rangle + |1\rangle)$ of its basis states and application of suitable control pulses leads to the entangled box–resonator superposition state $\frac{1}{\sqrt{2}}(|0\rangle|P_0\rangle + |1\rangle|P_1\rangle)$, where $|P_0\rangle$ and $|P_1\rangle$ are two distinguishable center-of-mass positions of the resonator.

oscillator. In essence, $\Delta x_{\rm zp}$ represents the quantum limit to position detection. For typical resonators, $\Delta x_{\rm zp}$ is on the order of only a tenth of a picometer [15]! Remarkably, recent experiments have managed to detect displacements of the nanomechanical resonator within just a few times of $\Delta x_{\rm zp}$ [16], thus approaching quantum-limited position measurements (with many existing applications to high-precision metrology, such as ultrasensitive mass and force detection [17]).

The other, from a foundational point of view even more exciting, application of QEMS is their potential to act as mechanical, macroscopic quantum systems. In the near future, it may be possible to prepare nanomechanical resonators in position-space superposition states and to observe the gradual decoherence of such states [18]. The idea of entangling macroscopically separated resonators has also been worked out in quite some detail [19], nourishing hopes that QEMS could potentially be used as mechanical qubits in quantum computers [20]. Given the enormous recent progress in fabricating QEMS in the laboratory, QEMS are likely to become major tools for explorations of the quantum-to-classical transition and the ultimate limits of quantum mechanics. What makes QEMS particularly interesting for this task is the fact that they are purely mechanical structures that are much more closer to the objects of the every-day world around us than the rather "artifical" systems considered, e.g., in experiments employing SQUIDs or Bose–Einstein condensates (BECs). Mechanical "Schrödinger kittens" in QEMS would correspond to spatial superposition states for macroscopic "rough" ordinary-matter mechanical objects composed of billions of atoms, perturbed by defects, imperfections, etc.

In the following, I will first discuss some important aspects related to the creation of spatial superposition states in QEMS (Sec. 2). I will then address the question of decoherence in QEMS. In particular, I will describe the need for the study of a new "canonical" decoherence model and summarize some first results (Sec. 3). To conclude this introduction, let me also point the reader to Blencowe's extensive review article on QEMS [15] which discusses some of the foundational issues associated with QEMS in greater detail than it has been possible in this paper. Shorter general-audience reviews of QEMS can be found, e.g., in [21, 22].

2. QEMS superposition states

2.1. A possible scheme

The basic idea for generating a superposition state involving two different spatial positions of the nanomechanical resonator is quite simple. We can use one of the several different existing qubit-type systems that are routinely prepared in the laboratory in coherent superpositions of their basis states $|0\rangle$ and $|1\rangle$. An example would be the Cooper-pair box, where the two basis states correspond to different values of electrical charge present on a superconducting island. A concrete scheme using such a Cooper-pair box has first been proposed by Armour, Blencowe, and Schwab [18] (see Fig. 2). If we add a thin layer of metal to the surface of the nanomechanical beam, the electrostatic interaction between the Cooper-pair box and the cantilever will lead to two different zero-point displacements of the beam (which we shall refer to as $|P_0\rangle$ and $|P_1\rangle$), depending on whether the box is in the charge state $|0\rangle$ or $|1\rangle$.

If we now prepare the box in a coherent superposition $\frac{1}{\sqrt{2}}(|0\rangle + |1\rangle)$ of its basis states and apply a suitable sequence of control pulses to the box, we can obtain an entangled box–resonator superposition state of the form $\frac{1}{\sqrt{2}}(|0\rangle|P_0\rangle + |1\rangle|P_1\rangle)$ involving the two center-of-mass position states $|P_0\rangle$ and $|P_1\rangle$ of the resonator. Provided the spatial separation between $|P_0\rangle$ and $|P_1\rangle$ is sufficiently macroscopic, we have thus created a state of the Schrödinger-cat type, with the resonator taking the place of the cat and the Cooper-pair box corresponding to the unstable atom in Schrödinger's original scheme.

2.2. The degree of "catness" of the superposition state

Let us discuss in some more detail to what extent such a spatial superposition state in QEMS may be considered truly "macroscopic" in the Schrödinger-cat sense. At the risk of stating the obvious, first of all it is very important to distinguish *macroscopic superpositions* from *superpositions of macroscopically distinct states*. The former type of superposition may simply refer to a macroscopic number N of (microscopic) particles in which each individual particle $i = 1, \ldots, N$ is in a (microscopic) superposition of its basis states $|0\rangle_i$ and $|1\rangle_i$: $|\Psi\rangle = \bigotimes_{i=1}^{N} \frac{1}{\sqrt{2}}(|0\rangle_i + |1\rangle_i)$. Clearly, this will in general not represent a cat state, which instead corresponds to a superposition of the quantum state corresponding to a macroscopic number of particles all being in the state $|0\rangle$ and a macroscopic number of particles all being in the state $|1\rangle$: $|\Psi\rangle = \frac{1}{\sqrt{2}}\left(\bigotimes_{i=1}^{N}|0\rangle_i + \bigotimes_{i=1}^{N}|1\rangle_i\right)$. The quantum state created by the scheme described in the previous Sec. 2.1 indeed falls into the second category. However, how do we quantify its "catness"?

There exist different sensible measures for this task, and we should here adhere to criteria initially proposed by Leggett [23, 24]. For a superposition of the form $|\Psi\rangle = \frac{1}{\sqrt{2}}\left(\bigotimes_{i=1}^{N}|0\rangle_i + \bigotimes_{i=1}^{N}|1\rangle_i\right)$ to qualify as a "cat" state, we require two conditions to be fulfilled. First, the component states $\bigotimes_{i=1}^{N}|0\rangle_i$ and $\bigotimes_{i=1}^{N}|1\rangle_i$ should differ by a large (macroscopic) amount in some extensive physical quantity relative to a suitably chosen microscopic reference value of this quantity (Leggett calls this measure "extensive difference"). In the case of QEMS, we may choose this quantity to be the separation between two resonator positions relative to the zero-point uncertainty displacement Δx_{zp}, where the latter corresponds to the order of magnitude of spatial resolution that is achievable in the read-out of the beam position. Second, generally, the number N of microscopic constituents (electrons, protons, neutrons) in the system should be macroscopic.

The second condition is certainly well satisfied for the nanomechanical resonators used in QEMS. Each resonator typically contains on the order of 10^9 atoms, and thus we may estimate $O(N) = 10^{10}$. The first condition of a large extensive difference, however, may not be as easily fulfilled. It will require more detailed and realistic estimates for the decoherence rate of spatial

Table 1. Estimates for the degree of macroscopic distinctness ("catness") of the components in QEMS position-space superpositions in comparison with other typical experiments. The seoncd column shows the difference in a characteristic extensive quantity, which is listed following the value and stated in units of a typical microscopic value (given in square brackets). The number of particles (third column) quantifies the physical "size" of the system in terms of the number of its microscopic constituents. Leggett [23, 24] argued that both measures should be large for a superposition to qualify as a cat state. The estimates for the experiments other than QEMS were obtained in [7].

Experiment	Extensive difference	Particle number
QEMS*	10 (separation [$\Delta x_{\rm zp}$])	10^{10}
SQUID	10^{10} (magnetic-moment diff. [$\mu_{\rm B}$])	10^9
C_{70}	10^6 (path separation [C_{70} size])	10^3
BEC*	10^7 (angular-momentum diff. [h])	10^9

*"Cat-like" superposition states not yet experimentally achieved

superposition states in QEMS to precisely pin down by what distance Δx we may be able to spatially separate the two components and still maintain reasonably long decoherence times to allow us to detect the superposition state. Using the (although probably inadequate) oscillator-bath model, Blencowe estimated a decoherence time between 0.1 and 1 μs for a separation Δx equal to a few times of the zero-point uncertainty displacement $\Delta x_{\rm zp}$ [15]. Since in this model the decoherence rate increases as $(\Delta x)^2$, a position-space separation of, say, $100\Delta x_{\rm zp}$ immediately puts us into the regime of decoherence times on the order of nanoseconds, which would presumably make it rather difficult to confirm the existence of the superposition state before its coherence is lost to the environment.

Although these numbers should be taken as very rough estimates only, it looks like that, within the current experimental capabilities and theoretical models, the achievable extensive difference for QEMS position-space superposition states will likely to be very limited – according to the values above, it will be on the order of about 10 (in terms of units of $\Delta x_{\rm zp}$). In Table 1, we compare the values of the two measures – extensive difference and number of microscopic constitutents – for QEMS superpositions with those obtained for other experiments involving superpositions of macroscopically distinct states, namely, SQUIDs, C_{70} interferometry, and BECs.

Given Leggett's conditions, the expected low extensive difference for QEMS makes it disputable whether such superpositions could legitimately be called "cat states." On the other hand, however, one may already regard the creation of a superposition involving two experimentally discernible positions of a macroscopic mechanical object as a significant step in its own right – an achievement that would correspond to the realization of a quantum state which is sufficiently "counterintuitive" to deserve being associated with the "Schrödinger cat" label. The author of this paper certainly agrees with this positive assessment. Furthermore, it is reasonable to anticipate that advances in experimental techniques will allow for an ever-improved shielding of decoherence and thereby allow for increasingly large separations in the beam-position superposition state that may greatly exceed the initial estimates mentioned here.

2.3. Could QEMS serve as a experimental test of physical collapse theories?

Angelo Bassi provided an excellent overview of collapse models at this conference, so I shall simply refer the reader to his contribution for an introduction to this topic. Whatever one's

opinion about the formal and physical viability and empirical and conceptual necessity of collapse models may be, they have one undisputable virtue: They are, at least in principle, experimentally falsifiable. Thus they go fundamentally beyond a mere interpretive rehash of quantum mechanics devoid of observable consequences.

The key challenge associated with tests of collapse models consists of creating a very peculiar experimental setting. On the one hand, the system must be sufficiently shielded from decoherence such that coherence would be expected to persist. On the other hand, the influence of the collapse mechanism on the state of the system must be strong enough to induce a reduction of the wavefunction. In other words, the decoherence rate must be reasonably lower than the physical localization rate. Currently there are no experiments that would meet this challenge [24, 25, 26, 27, 28, 29, 30, 7, 13].

Are QEMS suitable prospective candidates for experimental tests of physical collapse models? Let us shed some light on this issue through a simple numerical estimate (see also [15]). In the well-known GRW model [31], the characteristic localization timescale is $\tau_{\rm loc} = N^{-1} \times 10^{16}$ s, where N is the number of particles in the system. In QEMS, the beam consists of on the order of 10^9 atoms. Regardless of whether we take this number as an estimate for the particle number N or instead use the corresponding number of subatomic constituents (which increases N by about an order of magnitude), the resulting localization time is very slow, on the order of $\tau_{\rm loc} = 10^6$-10^7 s.

This number is to be compared with the typical decoherence time. In the GRW model, the localization mechanism becomes effective only once the two components in the spatial superpositions are separated by at least $\Delta = 100$ nm (which corresponds to the width of the Gaussian multiplying the wavefunction when a "hit" occurs). Therefore we would need to create a superposition of two positions of the nanomechanical beam at least Δ apart. In the previous section, we have already pointed out that, given the current experimental schemes and theoretical models, a separation of more than a few times of the zero-point uncertainty $\Delta x_{\rm zp}$ will be subject to decoherence on the nanosecond scale. With the reasonable estimate $\Delta x_{\rm zp} \sim 10^{-4}$ nm, we would need to achieve a separation on the order of $10^6 \Delta x_{\rm zp}$ for the localization to take place. Without any further calculation, it is clear that such a superposition would have an extremely short decoherence time, many orders of magnitude shorter than the localization time $\tau_{\rm loc} = 10^6$–10^7 s estimated above.

Therefore QEMS appear, at least currently, as rather poor candidates for testing physical collapse theories against standard quantum mechanics. It would require massively improved shielding of decoherence for QEMS to reach the domain in which such tests may become feasible. However, given the rapid evolution of QEMS and the somewhat flexible parameters and mechanisms underlying proposed collapse models, one should not be overly pessimistic. QEMS also have an important advantage over other experiments such as those using SQUIDs. The collapse is often tied to the mass density [32, 33, 34]; in particular, Penrose [35] has suggested that gravity may act as the ubiquituous collapse-inducing agent. Mechanical superposition states in QEMS would be directly susceptible to such collapse mechanisms. By contrast, in SQUIDs the superposition is composed of Cooper pairs (with decoherence acting in the current basis) and is essentially immune to the physical collapse [28, 29, 30, 7].

3. Decoherence and dissipation in QEMS

3.1. The physical nature of decoherence and dissipation in QEMS

Any success in the experimental generation of QEMS superposition states such as those described in Sec. 2 will fundamentally hinge on our ability to understand and control decoherence effects. Very little is known, both in terms of experimental data and of the appropriate theoretical formalism, about the relevant decoherence mechanisms and dynamics in QEMS. Since current experiments on QEMS have not yet achieved the controlled creation of superposition states,

experimental data is available only on dissipation in these systems, but not on decoherence. However, the theoretical expressions for, say, the dissipation rate (as obtained, e.g., from an appropriate master-equation formalism) are typically related to the expressions for the decoherence rate. Thus we are already in a position to test the predictions of decoherence models by checking them against the measured data on dissipation.

What, then, *is* currently known about decoherence and dissipation in QEMS? Without going into the finer details here, experimental evidence [36, 37] (see also earlier results in, e.g., [38, 39]) suggests that the main source of dissipation (and decoherence) in QEMS may be the interaction of the lowest fundamental flexural mode of the beam with a rather small number of defects in the beam itself. As we shall see in a second, this has interesting modeling implications. The defects effectively act as two-level systems and take various physical realizations. Important examples of such defects are charge traps, so-called elastic centers, impurity atoms (moving between two metastable positions), and dangling bonds due to the disruption of the crystal structure at the surface of the resonator. (It should be noted, however, that the exact physical nature of these two-level defects and the precise mechanism by which they interact with the beam's flexural mode is currently rather little understood, both experimentally and theoretically.)

This experimental evidence indicates that the appropriate model for describing dissipation and decoherence in QEMS may be of the *oscillator–spin type*, i.e., of a quantum harmonic oscillator (representing the fundamental mode of the beam) whose position coordinate is coupled to an environment of spin-1/2 particles (representing the two-level defects). An interesting question which we shall come back to below concerns the extent to which the defects themselves behave effectively classically due to *their* coupling to an environment – i.e., to what extent the model would need to incorporate further couplings of each spin-1/2 particle to another decohering bath to achieve a physically correct modeling of the two-level defects in the resonator.

Interestingly, the oscillator–spin model has received hardly any attention in the literature thus far, probably due to a lack of physical relevance before its applicability to QEMS was discovered. The bulk of existing research has been devoted to the three other "canonical" models for dissipation and decoherence: The oscillator-bath models, with the system either represented by an oscillator (quantum Brownian motion [40]) or a spin (spin–boson model [41]), and the spin–spin model of a central spin interacting with a bath of other spins [42]. Thus the oscillator–spin model is of interest both in the particular context of QEMS and within the broader scope of completing the family of canonical models.

Let us very briefly review some of the (sparse) literature on some aspects of the model. Motivated by the question of how the dissipation and decoherence dynamics change when the oscillator environment in the model for quantum Brownian motion is replaced by a spin environment, Caldeira et al. [43] considered a simplified version of the oscillator–spin model and solved it using the Feynman–Vernon influence technique [44] in the weak-coupling limit. They were able to show that the spin bath will in general lead to dynamics very different from those of the oscillator bath, but also that it is possible to match the oscillator-bath dynamics if one chooses a suitably modified spectral density for the spin bath. The latter result is not surprising: In their famous paper of 1963 Feynman and Vernon had already shown that, in the weak-coupling limit, *any* environment can be mapped onto an equivalent oscillator bath [44].

Other results related to the oscillator–spin model have been obtained in the context of a description of the acoustical properties of glasses, using models for interactions between phonon modes and two-level systems [45]. However, the application of these results is far from being able to consistently and rigorously explain the experimentally observed dissipation and decoherence properties in QEMS, especially in the low-temperature regime relevant to the (future) creation of superposition states and the observation of decoherence dynamics [37] (see also Fig. 3).

To the author's knowledge, there exist currently only two papers directly aimed at providing theoretical expressions for the dissipation rate in QEMS. Ahn and Mohanty [46] considered a

set of of two-level systems coupled to an acoustic wave and interacting with an environment of thermal phonons. They derived an expression for the total dissipation rate based on the total time-averaged phonon emission power of all two-level systems. Very recently (post-DICE 2006), Seoánez et al. [47] obtained an expression for the dissipation rate using Fermi's Golden Rule.

None of these treatments, though, derives a master equation (starting from the full resonator–bath Hamiltonian) for the reduced position-space density operator describing the center-of-mass position of the nanomechanical resonator under the influence of a dissipative environment of two-level defects. Some first steps in this direction have recently been undertaken by the author of this paper (in collaboration with Gerard Milburn) and shall be outlined in the following.

3.2. The "pure" oscillator–spin model

Let us first consider the most simple case in which the spins do not interact with any additional bath. That is, we consider the model of a single quantum harmonic oscillator (representing the resonator) coupled to a collection of spin-1/2 particles. We may call this configuration the "pure" oscillator–spin model or, in rather obvious terminology, the "inverse spin–boson model."

Let us introduce the relevant Hamiltonians. The harmonic oscillator has self-Hamiltonian $\hat{H}_{\mathcal{S}} = \frac{\hat{p}^2}{2m} + \frac{m\omega_0}{2}\hat{x}^2$ and interacts with a bath of N independent spin-1/2 particles with self-Hamiltonian

$$\hat{H}_{\mathcal{B}} \equiv \sum_{i=1}^{N} \hat{H}_{\mathcal{B}}^{(i)} = \sum_{i=1}^{N} \frac{\hbar\omega_i}{2}\hat{\sigma}_z^{(i)} + \sum_{i=1}^{N} \Delta_i \hat{\sigma}_x^{(i)}. \tag{1}$$

Here ω_i and Δ_i denote, respectively, the asymmetry (splitting) energy and tunneling matrix element of the ith bath spin. We take the spin bath to couple linearly to the position coordinate of the oscillator via the interaction Hamiltonian

$$\hat{H}_{\rm int} = \hat{x} \sum_{i=1}^{N} g_i \hat{\sigma}_z^{(i)} \equiv \hat{x}\hat{B}. \tag{2}$$

Thus the effect of the bath on the oscillator amounts to that of a (quantum) force. We shall also make the usual assumption assume that system and bath are initially uncorrelated, $\rho_{SB}(0) = \rho_{\mathcal{S}}(0) \otimes \rho_{\mathcal{B}}(0)$, with the bath being in thermal equilibrium, $\rho_{\mathcal{B}}(0) = \frac{1}{Z}\prod_{i=1}^{N} \mathrm{e}^{-\hat{H}_{\mathcal{B}}^{(i)}/k_{\rm B}T}$.

This model is quite general and not necessarily tied to QEMS. A physically meaningful application to QEMS would, among other things, require us to make appropriate choices for the parameters. In fact, parameters such as ω_i and Δ_i should not be expected to be static in the case of QEMS. Instead, the oscillatory motion of the beam, i.e., the strain induced by the phonons in the resonator, constantly deforms the potential landscape seen by each two-level system. One usually assumes that the dominant effect of this strain is to change the asymmetry energies ω_i of the defects.

The model defined by the sum of the Hamiltonians above is quite easily solved in the weak-coupling limit, such that standard second-order Feynman–Vernon theory [44] can be applied. Whether the weak-coupling limit is appropriate for QEMS remains to be seen. For now, the idea is simply to develop an initial model that can serve as a reasonable starting point and that can be confirmed or disproved by the experimental evidence.

Without giving the derivation here (which will be presented in a paper currently in preparation), let us mention some of the core results that come out of the solution of the oscillator–spin model in the weak-coupling limit. We find that the influence functional decomposes into two parts. The first term is time-independent and describes pure decoherence in the position basis with consequent momentum diffusion. The second term can be mapped onto the term obtained for the case of an oscillator bath in the following way. In the usual manner, one first goes from discrete environmental spins, indexed by i and described by parameters

(ω_i, Δ_i), to a continuum description in terms of a spectral density $J_{\rm spin}(\Omega)$ for the spin bath, where $\Omega = \sqrt{\omega^2 + \Delta^2}$ (dropping the index i since we are now working in the continuum limit). Then, if one chooses a new "effective" spectral density given by

$$J_{\rm eff}(\Omega, T) = J_{\rm spin}(\Omega) \tanh\left(\frac{\hbar\Omega}{2k_{\rm B}T}\right), \tag{3}$$

the second term appearing in the spin-bath influence functional becomes formally identical to that obtained for an oscillator bath with spectral density $J_{\rm eff}(\Omega, T)$. Thus, apart from the first pure-decoherence term, the influence functional for a spin bath with spectral density $J_{\rm spin}(\Omega)$ is (essentially) equivalent to that of an oscillator bath with a spectral density given by Eq. (3).

Therefore we can simply take over the results from the oscillator-bath model (i.e., from the model for quantum Brownian motion), including the master equation, but evaluated using the explicitly temperature-dependent spectral density (3). While this takes care of the second term in the spin-bath influence functional, the effect of the first (pure-decoherence) term can be accounted for by simply adding it to the relevant decoherence coefficients appearing in the oscillator-bath master equation [Eq. (4) below].

The resulting master equation for the reduced density operator $\hat{\rho}_{\mathcal{S}}$ of the resonator is thus of the form familiar from quantum Brownian motion [40],

$$\frac{d}{dt}\hat{\rho}_{\mathcal{S}} = \underbrace{-\frac{\rm i}{\hbar}\left[\hat{H}_0 + \frac{1}{2}m\widetilde{\omega}_0^2(t)\hat{x}^2, \hat{\rho}_{\mathcal{S}}\right]}_{\text{unitary evolution}} \underbrace{-\frac{{\rm i}\gamma(t)}{\hbar}\left[\hat{x}, \left\{\hat{p}, \hat{\rho}_{\mathcal{S}}\right\}\right]}_{\text{dissipation}} \underbrace{-D(t)\left[\hat{x}, \left[\hat{x}, \hat{\rho}_{\mathcal{S}}\right]\right] - \frac{f(t)}{\hbar}\left[\hat{x}, \left[\hat{p}, \hat{\rho}_{\mathcal{S}}\right]\right]}_{\text{decoherence}}. \tag{4}$$

Here $\gamma(t)$ is the dissipation coefficient, and $D(t)$ and $f(t)$ are, respectively, the normal and anomalous diffusion coefficients. These coefficients are strongly dependent on the particular form of the spectral density [40], leading to the (in general) significant differences in the system dynamics induced by oscillator baths vs. spin baths.

In particular, for the asymptotic value of the dissipation coefficient in the spin-bath case we find

$$\gamma(t \to \infty) \equiv \gamma(T) = \frac{1}{2m\omega_0} J_{\rm eff}(\omega_0, T) = \frac{1}{2m\omega_0} J_{\rm spin}(\omega_0) \tanh\left(\frac{\hbar\omega_0}{2k_{\rm B}T}\right), \tag{5}$$

where ω_0 is the resonator frequency. In contrast with the dissipation coefficient in the oscillator-bath case, this spin-bath dissipation coefficient is explicitly temperature-dependent. Interestingly, and maybe at a first glance counterintuitively, $\gamma(T)$, and thus the dissipation rate, *decreases* with increasing temperature. However, this behavior is rather easily explained. For an oscillator bath, each oscillator possesses an infinity of energy levels, so there is no upper limit to the amount of energy that can be absorbed by the bath. By contrast, a spin-1/2 particle has only two possible energy levels, so the spin bath as a whole saturates very quickly as the temperature (and thus the amount of energy that can be absorbed from the system) is increased. It follows that, since the dissipation rate of the oscillator bath (in the model for quantum Brownian motion) is temperature-independent, the ability of the spin bath to exert a dissipative effect on the system must *decrease* with increasing temperature. Indeed, the $\tanh(\hbar\omega_0/2k_{\rm B}T)$ temperature dependence of the dissipation rate as predicted by Eq. (5) has been observed experimentally in physical systems such as glasses [48] where dissipation is also due to interaction of phonon modes with two-level systems.[1]

How does the theoretical prediction (5) match the experimental data on QEMS? Fig. 3 shows measurements of the dissipation rate in QEMS for two different temperature regimes. Contrary

[1] The author is grateful to Miles Blencowe for drawing his attention to reference [48].

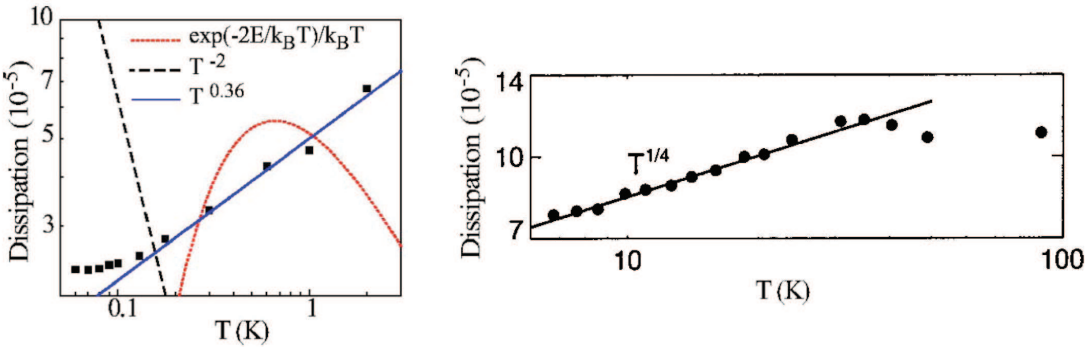

Figure 3. Experimental data on the dissipation rate of nanomechanical resonators as a function of temperature. The square dots (■) in the left plot show measurements taken by Zolfagharkhani et al. [37] in the low-T regime. The solid (——) blue line is the best power-law fit to the data, $\propto T^{-0.36}$. The dotted (· · · · · ·) red and dashed (- - - -) black lines are theoretical predictions from two existing models for the acoustic dissipation in crystals due to two-level systems in the low-temperature and high-temperature regime, respectively (see [37] for details). The poor agreement between this theory and the experiment can be clearly seen. The circles (●) in the right plot show data obtained by Mohanty et al. [36] for higher temperatures up to 100 K. The solid line (——) represents a power-law fit of the data, $\propto T^{1/4}$.

to the prediction of the pure oscillator–spin model, the measured dissipation rates are observed to *increase* with temperature. This strongly indicates that at least some of the two-level defects in the resonator should not be regarded as – apart form their coupling to the resonator – isolated quantum-coherent spin-1/2 particles, but instead as strongly coupled to an additional decohering and dissipative environment. This environment renders the tunneling of the spins incoherent and leads to relaxation of the spins. By absorbing the excess energy from the spin bath it prevents the spin bath from saturating.

3.3. The oscillator–spin–oscillator model

The results of the previous section suggest that the physically more appropriate model for decoherence and dissipation in QEMS may be (at the risk of abusing the nomenclature) the *oscillator–spin–oscillator model*, i.e., a quantum harmonic oscillator (the resonator) coupled to a – possibly quite small [37] – number of spin-1/2 particles (the two-level defects), each of which is in turn coupled to a dissipative boson bath. That is, we can treat the problem as that of a harmonic oscillator coupled to a collection of independent environmental systems, each of which corresponds to the familiar spin–boson model [41, 49]. We shall not discuss this model in any greater detail here, mainly, because studies of it are still in their infancy. In general, one could imagine taking into account the influence of the additional dissipative bath in two ways.

Following a rather phenomenological and less rigorous approach, we may simply augment the effective spectral density (3) for the spin bath with a prefactor that represents the temperature-dependent ralaxation of the spins due to the additional bosonic bath. This prefactor takes the typical form $\frac{\Omega\tau(T)}{1+\Omega^2\tau^2(T)}$ [49], where $\tau(T)$ is the (temperature-dependent) spin–boson relaxation time (with $d\tau(T)/dT < 0$). Thus the new effective spectral density is

$$J_{\rm eff}(\Omega,T) = J_{\rm spin}(\Omega)\frac{\Omega\tau(T)}{1+\Omega^2\tau^2(T)}\tanh\left(\frac{\hbar\Omega}{2k_{\rm B}T}\right), \qquad (6)$$

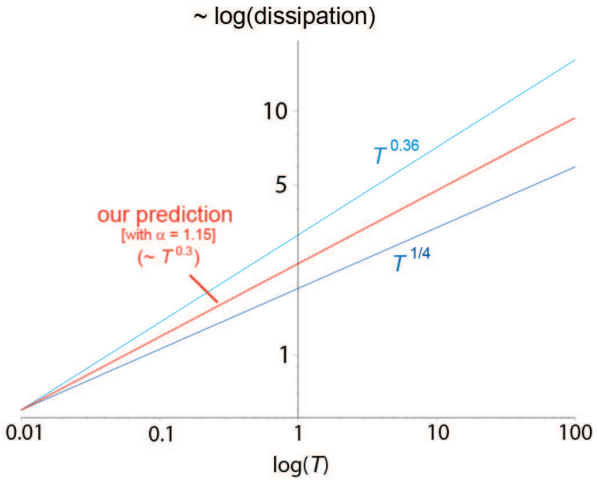

Figure 4. Temperature dependence of the dissipation rate predicted by Eq. (7) (red line), with $\tau(T) \propto T^{-2\alpha-1}$ and the choice $\alpha = 1.15$. The light and dark blue lines are the power-law fits of the experimental data shown in Fig. 3. Note that the units on the vertical axis do not correspond to physically meaningful values: All three lines were artifically made to coincide at $\log(T) = 0.01$ in order to clearly visualize the different power-law dependencies.

and the dissipation rate $\gamma(T)$, Eq. (5), now takes the form

$$\gamma(T) = \frac{1}{2m\omega_0} J_{\rm spin}(\omega_0) \frac{\omega_0 \tau(T)}{1 + \omega_0^2 \tau^2(T)} \tanh\left(\frac{\hbar\omega_0}{2k_{\rm B}T}\right). \tag{7}$$

A typical form of $\tau(T)$ derived in the context of the spin–boson model for an ohmic bosonic bath with strong coupling is $\tau(T) \propto T^{-2\alpha-1}$, with $\alpha \gtrsim 1$. If we choose, for example, $\alpha = 1.15$, we can match the experimentally observed temperature dependence of the dissipation rate in QEMS rather well (Fig. 4).

However, in the absence of further theoretical and experimental insights, there is quite some freedom in the choice of the parameters, and thus the approach of modeling the influence of spin-bath relaxation via the effective spectral density (7) may be considered as having a rather unsatisfying *ad hoc* character. It would therefore be more desirable to start from first principles and derive the master equation for the oscillator–spin–oscillator model, starting from the full microscopic Hamiltonian for the central oscillator interacting with a collection of spins (or, to start, even just a single spin) coupled to oscillator baths. Currently, this remains work in progress (carried out in collaboration with Gerard Milburn and Miles Blencowe).

Several other important questions beg for an answer. Is the weak-coupling approximation physically realistic in the case of QEMS? Do interactions *between* the spins in the bath need to be taken into account (e.g., to model the mechanism of "cooperative emission" [46])? How do the characteristics of decoherence and dissipation change if the resonator is driven into the nonlinear regime (given that it is in fact *difficult* to remain in the linear domain in experiments on QEMS)? QEMS offer a great array of new and interesting problems in the area of open quantum systems, and we are only at the very beginning of finding solutions and answers.

4. Outlook

A great feature of every DICE conference is that the meeting brings together physicists from very diverse scientific backgrounds but with a shared passion for the fundamentals and

foundations of physics. QEMS would appear to constitute an ideal new object of interest to this community. All the intrincate engineering-type challenges associated with the practical realization of these systems aside, QEMS provide an exciting and promising arena for the experimental and theoretical exploration of foundational questions in the context of macroscopic, purely mechanical systems as close to "every-day" objects as one could currently hope for.

With fields such as quantum computing having now become rather crowded, the area of QEMS is refreshingly novel and offers plenty of room for future ground-breaking work, both in the experimental and theoretical domain. The oscillator–spin model for decoherence discussed in this paper provides an excellent example for the great potential inherent in the field of QEMS. In spite of being a member of the set of four canonical decoherence models, this model has hitherto hardly been studied. Now, as QEMS have provided a physical justification for the consideration of the model, further studies (especially when generalized to the oscillator–spin–oscillator model described in Sec. 3.3) will not only enhance our theoretical understanding of fundamental aspects of decoherence, but also ultimately allow us to experimentally distinguish and test the predictions of different canonical decoherence models (oscillator vs. spin baths, spin baths coupled to a dissipative bath, etc.).

The future for QEMS and their role in the foundations of quantum mechanics looks bright. The next couple of years will certainly present us with breathtaking new experimental achievements and theoretical breakthroughs in the field, so let us look forward to DICE 2008!

Acknowledgments

The work described in Sec. 3 was carried out in collaboration with Gerard Milburn. We thank Miles Blencowe and Ross McKenzie for helpful discussions.

References

[1] Schrödinger E 1935 *Naturwissenschaften* **23** 807–12, 823–28, 844–49
[2] Friedman J R, Patel V, Chen W, Yolpygo S K and Lukens JE 2000 *Nature* **406** 43–6
[3] van der Wal C H, ter Haar A C J, Wilhelm F K, Schouten R N, Harmans C J P M, Orlando T P, Lloyd S and J. E. Mooij J E 2000 *Science* **290** 773–7
[4] Arndt M, Nairz O, Vos-Andreae J, Keller C, van der Zouw G and Zeilinger A 1999 *Nature* **401** 680–2
[5] Brezger B, Hackermüller L, Uttenthaler S, Petschinka J, Arndt M and Zeilinger A 2002 *Phys. Rev. Lett.* **88** 100404
[6] Hackermüller L, Uttenthaler S, Hornberger K, Reiger E, Brezger B, Zeilinger A and Arndt M 2003 *Phys. Rev. Lett.* **91** 090408
[7] Schlosshauer M 2006 *Ann. Phys.* **321** 112–49
[8] Zeh H D 1970 *Found. Phys.* **1** 69–76
[9] Zeh H D 1973 *Found. Phys.* **3** 109–16
[10] Zurek W H 1981 *Phys. Rev. D* **24** 1516–25
[11] Zurek W H 2003 *Rev. Mod. Phys.* **75** 715–75
[12] Joos E, Zeh H D, Kiefer C, Giulini D, Kupsch J and Stamatescu I O 2003 *Decoherence and the Appearance of a Classical World in Quantum Theory* (New York: Springer)
[13] Schlosshauer M 2004 *Rev. Mod. Phys.* **76** 1267–1305
[14] Henry Huang X M, Zorman C A, Mehregany M and Roukes M L 2003 *Nature* **421** 496
[15] Blencowe M P 2004 *Phys. Rep.* **395** 159–222
[16] LaHaye M D, Buu O, Camarota B and Schwab K C 2004 *Science* **304** 74–7
[17] Ekinci K L, Yang Y T and Roukes M L 2004 *J. Appl. Phys.* **95** 2682–9
[18] Armour A D, Blencowe M P and Schwab K C 2002 *Phys. Rev. Lett.* **88** 148301
[19] Eisert J, Plenio M B, Bose S and Hartley J 2004 *Phys. Rev. Lett.* **93** 190402
[20] Savel'ev S, Hu X and Nori F 2004 Quantum electromechanics: Qubits from buckling nanobars *Preprint* cond-mat/0412521.
[21] Schwab K C and Roukes M L 2005 *Phys. Today* (July 2005) 36–42
[22] Roukes M L 2001 *Phys. World* **14** 25–31
[23] Leggett A J 1980 *Suppl. Prog. Theor. Phys.* **69** 80–100
[24] Leggett A J 2002 *J. Phys.: Condens. Matter* **14** R415–51

[25] Adler S L 2004 *Quantum Theory as an Emergent Phenomenon* (Cambridge, UK: Cambridge University Press) chapter 6.5
[26] Benatti F, Ghirardi G C and Grassi R *Quantum mechanics with spontaneous localization and experiments* (Advances in Quantum Phenomena) ed E G Beltrametti and J M Lévy-Leblond (New York: Plenum) pp 263–79
[27] Bassi A, Ippoliti E and Adler S L 2005 *Phys. Rev. Lett.* **94** 030401
[28] Rae A I M 1990 *J. Phys. A* **23** L57–60
[29] Buffa M, Nicrosini O and Rimini A 1995 *Found. Phys. Lett.* **8** 105–25
[30] Bassi A and Ghirardi G C 2003 *Phys. Rep.* **379** 257–426
[31] Ghirardi G C, Rimini A and Weber T 1986 *Phys. Rev. D* **34** 470–91
[32] Diósi L 1989 *Phys. Rev. A* **40** 1165–74
[33] Pearle P 1989 *Phys. Rev. A* **39** 2277–89
[34] Ghirardi G C, Pearle P and Rimini A 1990 *Phys. Rev. A* **42** 78–89
[35] Penrose R 1989 *The Emperors New Mind* (Oxford, UK: Oxford University Press)
[36] Mohanty P, Harrington D A, Ekinci K L, Yang Y T, Murphy M J and Roukes M L 2002 *Phys. Rev. B* **66** 085416
[37] Zolfagharkhani G, Gaidarzhy A, Shim S B, Badzey R L and Mohanty P 2005 *Phys. Rev. B* **72** 224101
[38] Kleiman R N, Agnolet G and Bishop D J 1987 *Phys. Rev. Lett.* 2079–82
[39] Mihailovich R E and Parpia J M 1992 *Phys. Rev. Lett.* **68** 3052–55
[40] Hu B L, Paz J P and Zhang Y 1992 *Phys. Rev. D* **45** 2843–61
[41] Leggett A J, Chakravarty S, Dorsey A T, Fisher M P A and Garg A 1987 *Rev. Mod. Phys.* **59** 1–85
[42] Prokof'ev N V and Stamp P C E 2000 *Rep. Prog. Phys.* **63** 669–726
[43] Caldeira A O, Castro Neto A H and Oliveira de Carvalho T 1993 *Phys. Rev. B* **48** 13974–76
[44] Feynman R P and Vernon F L 1963 *Ann. Phys. (N.Y.)* **24** 118–73
[45] Phillips W A 1987 *Rep. Prog. Phys.* **50** 1657–708
[46] Ahn K H and Mohanty P 2003 *Phys. Rev. Lett.* **90** 085504
[47] Seoanez C, Guinea F and Castro Neto A H 2006 Dissipation due to two-level systems in nano-mechanical devices *Preprint* cond-mat/0611153
[48] Golding B, Graebner J E and Schutz R J 1976, *Phys. Rev. B* **14** 1660–2
[49] Weiss U 1999 *Quantum Dissipative Systems* (Singapore: World Scientific)